A Circuit Reduction Technique for Finding the Steady-State Solution of Nonlinear Circuits

Emad Gad, *Student Member, IEEE*, Roni Khazaka, *Student Member, IEEE*, Michel S. Nakhla, *Fellow, IEEE*, and Richard Griffith, *Student Member, IEEE*

***Abstract*—Computing the steady-state response of large nonlinear circuits is becoming a key simulation requirement due to the rapid market growth of RF silicon integrated circuits. In this paper, we describe a nonlinear circuit reduction algorithm for finding the steady-state response. The proposed algorithm uses a congruent transformation-based technique to reduce the harmonic-balance equations into a much smaller set of equations. The main feature of the reduced circuit is that it shares with the original one a certain number of the derivatives with respect to the RF input power. Steady-state analysis is then done on the reduced circuit instead of the original circuit.**

***Index Terms*—Circuit reduction, harmonic balance, Krylov projection, nonlinear circuits, steady-state response.**

I. Introduction

THE rapid growth in RF silicon integrated circuits (ICs) for mobile communication systems has placed new demands on the simulation tools. Quantities such as intermodulation and harmonic distortion are typically of interest to circuit designers. However, finding the steady-state response for large analog and microwave nonlinear circuits represents an increasing challenge. The reason for this is that these circuits usually exhibit characteristics that make most traditional transient-based time-domain approaches perform poorly. For instance, if there are widely separated time constants in the circuit, then the usual transient analysis can take many clock cycles before the steady-state solution is reached.

The harmonic-balance (HB) technique [1], [2] has been introduced to address the above difficulties. The main philosophy behind HB by is that waveforms in a periodically excited nonlinear circuit are periodic and, thus, can be represented in the frequency domain as a finite Fourier series. In effect, this transforms the differential equations describing the circuit into a set of nonlinear algebraic equations that can be solved directly using iterative techniques such as the Newton–Raphson (NR) method. However, the main bottleneck that comes with solving this set of nonlinear equations is the prohibitive CPU cost that is required to store and factorize the Jacobian matrix of the nonlinear equations. Unfortunately, for large RF ICs with strong nonlinearities, this Jacobian matrix becomes large and dense [3] and its factorization can be expensive even for medium-sized circuits [5]. In addition, like all other locally convergent methods, NR has convergence problems. Convergence can be achieved only by finding sufficiently close initial values to the solution, which is difficult, particularly for the cases of high excitation levels. Continuation methods, on the other hand, have been proposed to avoid the convergence problems associated with the direct NR method. In the continuation methods scheme, the original set of nonlinear equations is replaced with an auxiliary system of the same size whose solution is trivial, and then use some sweeping parameter to trace the solution trajectory back to the original system. However, these methods are computationally expensive as they require the factorization of the Jacobian matrix at many values of the sweeping parameter. In addition, matrix-implicit linear solvers have been introduced to reduce the high cost of factorizing and storing the Jacobian matrix. In this scheme, only the components of the Jacobian matrix need to be stored and Krylov-subspace iterative solvers are used [4]. However, these methods require the use of preconditioners to improve their convergence. In addition, they still need to operate on the full size of the Jacobian matrix.

In this paper, we describe a new algorithm that poses the problem from a different perspective. The crux of the proposed algorithm is to reduce the size of the Jacobian matrix needed for the HB solution quite drastically, through the introduction of the new concept of nonlinear circuit reduction. This enables the original large set of nonlinear equations representing the HB equations to be replaced with a much smaller set of nonlinear equations. The main feature of the reduced set is that it shares with the original one the first few derivatives with respect to the RF excitation level at the dc operating point. A continuation scheme is then used to trace the solution of the reduced equations and map it back to the space of the original circuit equations. This introduces a significant computational advantage, as the size of the Jacobian matrix that needs to be factorized is typically much smaller than the size of the original Jacobian.

The organization of this paper is as follows. Section II provides a brief description of the HB approach. Sections III and IV describe the proposed algorithm and computation of the derivatives, respectively. Section V gives a proof for the equivalence of the derivatives between the reduced and original systems. Numerical examples and conclusion are described in Sections VI and VII, respectively.

II. HB Approach

Consider a circuit consisting of nonlinear and linear components. Using a nodal approach, Kirchoff's current laws can be

Manuscript received March 7, 2000; revised August 22, 2000.

The authors are with the Department of Electronics, Carleton University, Ottawa, ON, Canada K1S 5B6.

Publisher Item Identifier S 0018-9480(00)10733-1.

used to describe the circuit as [2]

$$\int_{-\infty}^{t} \boldsymbol{y}(t-\tau)\boldsymbol{x}(\tau)\,d\tau + \boldsymbol{i}(\boldsymbol{x}(t)) + \frac{d}{dt}\boldsymbol{q}(\boldsymbol{x}(t)) + \boldsymbol{i}_s(t) = 0 \tag{1}$$

where

$\boldsymbol{y}(t) \in \Re^{N\times N}$	impulse response matrix of the linear components;
$\boldsymbol{x}(t) \in \Re^{N}$	vector containing the nodes voltage waveforms;
$\boldsymbol{i}_s(t) \in \Re^{N}$	vector containing the Norton equivalents of the source voltage waveforms [7];
$\boldsymbol{i}(\boldsymbol{x}) \in \Re^{N}$ and $\boldsymbol{q}(\boldsymbol{x}) \in \Re^{N}$	functions describing the nonlinear conductances and capacitances in the circuit, respectively;
N	total number of nodes in the circuit.

The HB approach assumes that $\boldsymbol{x}(t)$, $\boldsymbol{i}(\boldsymbol{x}(t))$, $\boldsymbol{q}(\boldsymbol{x}(t))$, and $\boldsymbol{i}_s(t)$ can be written as a finite Fourier series, i.e.,

$$\boldsymbol{x}(t) = \sum_{k=-H}^{H} \boldsymbol{X}_k e^{jk\omega_o t} \tag{2}$$

$$\boldsymbol{i}(t) = \sum_{k=-H}^{H} \boldsymbol{I}_k e^{jk\omega_o t} \tag{3}$$

$$\boldsymbol{q}(t) = \sum_{k=-H}^{H} \boldsymbol{Q}_k e^{jk\omega_o t} \tag{4}$$

$$\boldsymbol{i}_s(t) = \sum_{k=-H}^{H} \boldsymbol{I}_{s,k} e^{jk\omega_o t} \tag{5}$$

where $\boldsymbol{X}_k$, $\boldsymbol{I}_k$, $\boldsymbol{Q}_k$, and $\boldsymbol{I}_{s,k}$ represent the harmonics for the nodes voltages, currents of the nonlinear conductances, charge of the nonlinear capacitances and sources currents, respectively, and ω_o is the fundamental frequency. Thus, (1) can be rewritten in the frequency domain as the following set of nonlinear equations:

$$\boldsymbol{F}(\boldsymbol{X}) \equiv \boldsymbol{Y}\boldsymbol{X} + \boldsymbol{I}(\boldsymbol{X}) + j\Omega\boldsymbol{Q}(\boldsymbol{X}) + \boldsymbol{I}_s = 0 \tag{6}$$

where $\boldsymbol{Y}$ is an $N(2H+1)\times N(2H+1)$ complex block matrix, i.e., $\boldsymbol{Y} = [\boldsymbol{Y}_{ij}]$, whose block matrices $\boldsymbol{Y}_{ij}$ are given by

$$\boldsymbol{Y}_{ij} = \operatorname{diag}\big[\Upsilon_{ij}(jk\omega_o)\big], \qquad k = -H, \ldots, 0, \ldots, H \tag{7}$$

where $\Upsilon(j\omega)$ is the $\boldsymbol{Y}$-parameters matrix of the linear components. In (6) Ω is a diagonal matrix such that it has N cycles of $(-H\omega_o, \ldots, 0, \ldots, H\omega_o)$ along its main diagonal and $\boldsymbol{X}$ is $N(2H+1)\times 1$ vector that contains the harmonics for the voltage waveforms at the N nodes. Solving the system of nonlinear equations (6) will be explored in Sections II-A and II-B.

A. Newton–Raphson Method

In the Newton–Raphson (NR) method, the harmonics solution vector is updated iteratively in the following way:

$$\boldsymbol{X}^{n+1} = \boldsymbol{X}^{n} - \boldsymbol{J}(\boldsymbol{X}^{n})^{-1}\boldsymbol{F}(\boldsymbol{X}^{n}) \tag{8}$$

where $\boldsymbol{J}(\boldsymbol{X}^n)$ is the Jacobian matrix of $\boldsymbol{F}$ with respect to $\boldsymbol{X}$

$$\boldsymbol{J}(\boldsymbol{X}^{n}) = \left.\frac{d\boldsymbol{F}}{d\boldsymbol{X}}\right|_{\boldsymbol{X}=\boldsymbol{X}^n} = \left.\left(\frac{d\boldsymbol{I}}{d\boldsymbol{X}} + j\Omega\frac{dQ}{d\boldsymbol{X}}\right)\right|_{\boldsymbol{X}=\boldsymbol{X}^n} + \boldsymbol{Y}. \tag{9}$$

Here, the matrix $(d\boldsymbol{I}/d\boldsymbol{X})$ can be represented in the block form

$$\frac{d\boldsymbol{I}}{d\boldsymbol{X}} = [\boldsymbol{L}_{mn}], \qquad m, n = 1, 2, \ldots, N \tag{10}$$

where the (k, l) entry in the blocks $\boldsymbol{L}_{mn}$ is given by

$$[\boldsymbol{L}_{mn}]_{kl} = \frac{1}{T_o}\int_0^{T_o} \frac{\partial}{\partial v_n(t)}\, i_m(t) \exp\big(-j(k-l)\omega_o t\big) \tag{11}$$

where T_o is the fundamental period, i.e., $T_o = 2\pi/\omega_o$. The entries for the matrix $dQ/d\boldsymbol{X}$ are similar to those of $d\boldsymbol{I}/d\boldsymbol{X}$ in (11).

As can be seen here, the major time-consuming part is spent in factorizing the Jacobian matrix due to its large size and dense structure.

In addition, it is widely known that the NR method is locally convergent. Thus, convergence can be very fast only if the starting point is sufficiently close to the solution. Otherwise the method diverges.

B. Continuation Methods

Continuation methods are usually used to overcome the convergence problems associated with the iterative techniques such as the NR method described above. The basic idea of the continuation methods is to augment the system $\boldsymbol{F}(\boldsymbol{X})$ in (6) with some parameter, say, α, to obtain another auxiliary system $\psi(\boldsymbol{X}, \alpha)$. Here, α is chosen such that the system given by $\psi(\boldsymbol{X}, 0)$ has a trivial solution in $\boldsymbol{X}$ and the system given at $\psi(\boldsymbol{X}, 1) = \boldsymbol{F}(\boldsymbol{X})$ identically in $\boldsymbol{X}$. For our case, the augmented system can be formulated by splitting the source vector $\boldsymbol{I}_s$ into two vectors and writing down the new system as

$$\psi(\boldsymbol{X}, \alpha) \equiv \boldsymbol{Y}\boldsymbol{X} + \boldsymbol{I}(\boldsymbol{X}) + j\Omega\boldsymbol{Q}(\boldsymbol{X}) + \boldsymbol{I}_{\mathrm{dc}} + \alpha\boldsymbol{I}_t = \boldsymbol{0}. \tag{12}$$

Here, $\boldsymbol{I}_t$ is a vector that represents the harmonics due to the RF sources in the circuit, while $\boldsymbol{I}_{\mathrm{dc}}$ represents the biasing dc sources. At $\alpha = 0$, the solution of (12) is simply the solution obtained from the usual dc analysis, while at $\alpha = 1$, the system $\psi(\boldsymbol{X}, 1)$ has the same solution as (6). Thus, a typical continuation method proceeds by taking small increments in α and solving the system $\psi(\boldsymbol{X}, \alpha)$, until $\alpha = 1$.

Although the continuation methods have provided a major advantage in being able to avoid the convergence problems, they are computationally expensive because they require the solution of many auxiliary systems of equations corresponding to various values of α. In addition, the major time consuming part spent in factorizing the large and dense Jacobian still dominates the computation.

III. Proposed Algorithm

The main objective of the proposed algorithm is to significantly reduce the size of the original circuit described in (1)

and, consequently, the size of the Jacobian matrix. This is done by replacing the original large set of equations in (12) by a much smaller one. The reduced set of equations is obtained by effecting the following change of variables:

$$\boldsymbol{X} \rightarrow \boldsymbol{V}\hat{\boldsymbol{X}} \tag{13}$$

in (12), and then premultiplying by $\boldsymbol{V}^T$ to obtain the new set of equations given by

$$\hat{\psi}(\boldsymbol{X}, \alpha) \equiv \hat{\boldsymbol{Y}}\hat{\boldsymbol{X}} + \boldsymbol{V}^T\boldsymbol{I}(\boldsymbol{V}\hat{\boldsymbol{X}}) + j\boldsymbol{V}^T\,\Omega\boldsymbol{Q}(\boldsymbol{V}\hat{\boldsymbol{X}}) + \hat{\boldsymbol{I}}_{\rm dc} + \alpha\hat{\boldsymbol{I}}_t = 0 \tag{14}$$

where

$$\hat{\boldsymbol{Y}} = \boldsymbol{V}^T\boldsymbol{Y}\boldsymbol{V} \quad \hat{\boldsymbol{I}}_{\rm dc} = \boldsymbol{V}^T\boldsymbol{I}_{\rm dc} \quad \hat{\boldsymbol{I}}_t = \boldsymbol{V}^T\boldsymbol{I}_t. \tag{15}$$

In the above equation, $\boldsymbol{V} \in \Re^{N(2H+1)\times q}$ is an orthonormal basis for the subspace spanned by the first q Taylor's series coefficients (or the scaled derivatives) of $\boldsymbol{X}$ with respect to α with $q \ll N(2H+1)$. In other words, if the Taylor series expansion of $\boldsymbol{X}$ with respect to α is given as

$$\boldsymbol{X} = \sum_{k=0}^{\infty} \boldsymbol{A}_k(\alpha - \alpha_{\rm o})^k \tag{16}$$

then

$$\mathrm{colspan}(\boldsymbol{V}) = \mathrm{colspan}(\boldsymbol{A}_{\rm o}, \boldsymbol{A}_1, \ldots, \boldsymbol{A}_{q-1}). \tag{17}$$

The basic concept behind this change of variables is that the reduced system obtained by this transformation preserves the first q Taylor's series coefficients of the original system under the mapping $\boldsymbol{V}$ [8]. More precisely, if $\hat{\boldsymbol{X}}$ is expanded as the Taylors' series

$$\hat{\boldsymbol{X}} = \sum_{k=0}^{\infty} \hat{\boldsymbol{A}}_k(\alpha - \alpha_{\rm o})^k \tag{18}$$

then

$$\boldsymbol{A}_k = \boldsymbol{V}\hat{\boldsymbol{A}}_k, \qquad k = 0, \ldots, q-1. \tag{19}$$

In this case, applying the continuation method to the system in (14) to track the solution trajectory requires the factorization of the $q \times q$ Jacobian matrix

$$\hat{\boldsymbol{J}} = \boldsymbol{V}^T\left(\frac{d\boldsymbol{I}}{d\boldsymbol{X}} + j\Omega\frac{d\boldsymbol{Q}}{d\boldsymbol{X}} + \boldsymbol{Y}\right)\boldsymbol{V}. \tag{20}$$

This provides a significant computational advantage since the size of the Jacobian in (20) is typically much smaller than the one in (9). Solutions in the space of the original circuit HB equations are thus obtained using the mapping in (13).

Another computational advantage offered by (20) is that computing the reduced Jacobian does not require the original one to be constructed explicitly. To explain this fact, we use a permutation operator to rewrite (23) in the form [5]

$$\boldsymbol{J} = \boldsymbol{Y} + j\Omega\Gamma^{-1} + \Gamma\boldsymbol{G}\Gamma^{-1} \tag{21}$$

where Γ is the $(2H+1)$ discrete Fourier transform (DFT) operator and the matrices $\boldsymbol{C}$ and $\boldsymbol{G}$ are block diagonals with blocks representing the linearization of the circuit at the sampling time points t_s, $s = 1, \ldots, S$ with $S = 2H+1$. Thus, by exploiting the structure shown in (21), the reduced Jacobian in (20) can be constructed efficiently by a series of matrix vector products using the fast Fourier transform (FFT) [10]. Another advantage that can be seen from (20) is that the construction of the reduced Jacobian lends itself quite easily to parallel processing.

IV. Computation of the Derivatives

To compute the derivatives, we proceed by writing (12) in the form

$$\boldsymbol{Y}\boldsymbol{X} + \Phi(\boldsymbol{X}) + \boldsymbol{I}_{\rm dc} + \alpha\boldsymbol{I}_t = \boldsymbol{0} \tag{22}$$

where $\Phi(\boldsymbol{X}) = \boldsymbol{I}(\boldsymbol{X}) + j\Omega\boldsymbol{Q}(\boldsymbol{X})$ and then expanding both $\boldsymbol{X}$ and $\Phi(\boldsymbol{X})$ as a Taylor series in α

$$\boldsymbol{X}(\alpha) = \sum_{i=0} \boldsymbol{A}_i\alpha^i \quad \Phi\big(\boldsymbol{X}(\alpha)\big) = \sum_{i=0} \boldsymbol{D}_i\alpha^i. \tag{23}$$

Clearly, at $\alpha = 0$, we have $\Phi(\boldsymbol{X}(0)) = \boldsymbol{D}_0 = \Phi(\boldsymbol{A}_0)$. Substituting from (23) into (22) and setting $\alpha = 0$ results in

$$\boldsymbol{Y}\boldsymbol{A}_0 + \Phi(\boldsymbol{A}_0) + \boldsymbol{I}_{\rm dc} = \boldsymbol{0}. \tag{24}$$

Note that A_o in (24) is simply the dc solution. Also equating the first power of α yields

$$\boldsymbol{Y}\boldsymbol{A}_1 + \boldsymbol{D}_1 + \boldsymbol{I}_t = \boldsymbol{0}. \tag{25}$$

Now define $\boldsymbol{J}(\alpha)$ to be

$$\boldsymbol{J}(\alpha) = \frac{d\Phi}{d\boldsymbol{X}} \qquad \boldsymbol{J}_o = \boldsymbol{J}(\alpha)\big|_{\alpha=0}. \tag{26}$$

Since $\boldsymbol{D}_1 = (d\Phi/d\alpha)|_{\alpha=0} = (d\Phi/d\boldsymbol{X})\,\boldsymbol{A}_1$, then substituting in (25) gives the following relation for $\boldsymbol{A}_1$:

$$(\boldsymbol{Y} + \boldsymbol{J}_0)\boldsymbol{A}_1 = -\boldsymbol{I}_t. \tag{27}$$

In order to compute $\boldsymbol{A}_2, \ldots, \boldsymbol{A}_n$, we expand $\boldsymbol{J}(\alpha)$ as a Taylor's series in α

$$\boldsymbol{J}(\alpha) = \sum_{k=0} \boldsymbol{J}_k\alpha^k \tag{28}$$

and then use this expansion to write $d\Phi/d\alpha$ in the following form:

$$\frac{d\Phi}{d\alpha} = \boldsymbol{J}\frac{d\boldsymbol{X}}{d\alpha}$$
$$\sum_{i=1} i\boldsymbol{D}_i\alpha^{i-1} = \sum_{i=0} \boldsymbol{J}_i\alpha^i \sum_{i=1} i\boldsymbol{A}_i\alpha^{i-1}. \tag{29}$$

Taking the nth derivative in (29) with respect to α and putting $\alpha = 0$, we get the following recursive relationship:

$$\boldsymbol{D}_n = \boldsymbol{J}_0\boldsymbol{A}_n + \frac{1}{n}\sum_{j=1}^{n-1}(n-j)\boldsymbol{J}_j\boldsymbol{A}_{n-j}. \tag{30}$$

Thus, taking the nth derivative with respect to α in (29) and substituting $\alpha = 0$ results in

$$(\boldsymbol{Y} + \boldsymbol{J}_0)\boldsymbol{A}_n = -\frac{1}{n}\sum_{i=1}^{n-1}(n-j)\boldsymbol{J}_j\boldsymbol{A}_{n-j}. \tag{31}$$

It is clear from (27) and (31) that computing $\boldsymbol{A}_1, \ldots, \boldsymbol{A}_n$ requires only one LU decomposition of the Jacobian matrix and each derivative can be obtained by one forward/backward substitution. Next, we proceed to show how to compute the right-hand side in (31). The term $\boldsymbol{A}_{n-j}$ represents the derivatives with respect to α with $\boldsymbol{A}_0$ and $\boldsymbol{A}_1$ evaluated using (24) and (27), and the higher order $(n-j)$th derivative evaluated recursively using (31). The other term required in (31) is $\boldsymbol{J}_i$. For simplicity of presentation, we address only one of the nodes with nonlinear elements, but the method is general for any number of nonlinear elements in the network. Consider a nonlinear resistive element governed by the relation $i(x) = f(x)$. In this case

$$\boldsymbol{J} = \Gamma \boldsymbol{G} \Gamma^{-1} \tag{32}$$

with

$$\boldsymbol{G} = \operatorname{diag}\Big(g(x(t_1)), \ldots, g(x(t_S))\Big) \tag{33}$$

$$g(x) = \frac{\partial}{\partial x} f(x) \tag{34}$$

where $t_1 \ldots, t_S$ are time points over the fundamental period. Noting the Taylor expansions

$$\begin{aligned} x &= \sum_{i=0} \alpha_i \alpha^i \\ f(x) &= \sum_{i=0} d_i \alpha^i \\ g(x) &= \partial f / \partial x = \sum_{i=0} g_i \alpha^i \end{aligned} \tag{35}$$

we can write the expression for $\boldsymbol{J}_i$ as

$$\boldsymbol{J}_i = \Gamma \boldsymbol{G}_i \Gamma^{-1} \tag{36}$$

where $\boldsymbol{G}_i$ is a diagonal matrix whose elements are the time samples of g_i. As an example of computing g_i, consider the case where

$$f(x) = I_S\left(\exp\left(x/V_T\right) - 1\right) \quad g(x) = \frac{I_S}{V_T} \exp\left(x/V_T\right) \tag{37}$$

then it can be shown that

$$g_n = \frac{1}{n V_T} \sum_{i=0}^{n-1} g_j a_{n-j}(n-j). \tag{38}$$

Similar expansions can be found for other functions as shown in Table I [11].

TABLE I
SOME FORMULAS FOR THE DERIVATIVES OF SIMPLE FUNCTIONS

Equation	$y = \sum_{i=0} c_i \alpha^i$, $f = \sum_{i=0} d_i \alpha^i$, $z = \sum_{i=0} e_i \alpha^i$
$f = \exp(y)$	$d_0 = \exp(c_0)$ $d_n = (1/n)\sum_{i=0}^{n-1} d_i c_{n-i}(n-i)$
$f = \log(y)$	$d_0 = \log(c_0)$ $d_n = (1/c_0)(c_m - \sum_{i=1}^{n-1} d_{n-i} c_i((n-i)/n))$
$f = y^p$	$d_n = (p d_0 c_n n + \sum_{i=1}^{n-1} c_i d_{n-i}(i(p+1)-n))/n c_0$
$f = y + z$	$d_n = c_n + e_n$
$f = y - z$	$d_n = c_n - e_n$
$f = yz$	$d_n = \sum_{i=0}^{n} c_i e_{n-i}$
$f = y/z$	$d_n = (c_n - \sum_{i=0}^{n-1} d_i e_{n-i})/e_0$

V. PROOF OF DERIVATIVES PRESERVATION

In this section, we prove that the reduced system in (14) shares with the original set of equations in (12) the first q derivatives with respect to α. The proof will be given by *mathematical induction*. First, it shall be proven that the first derivative of $\hat{\boldsymbol{X}}$ with respect to α as obtained from the reduced equations in (14) is equivalent to the one obtained from the original HB equations in (12) through mapping by $\boldsymbol{V}$. Next, we proceed by showing that the same relation applies to the kth derivative of $\hat{\boldsymbol{X}}$ provided that the previous $(k-1)$ derivatives are preserved under using the mapping $\boldsymbol{V}$.

First, $\hat{\boldsymbol{X}}(\alpha)$, $\boldsymbol{I}(\boldsymbol{V}\hat{\boldsymbol{X}})$, and $\boldsymbol{Q}(\boldsymbol{V}\hat{\boldsymbol{X}})$ in (14) are expanded in Taylor series form

$$\begin{aligned} \hat{\boldsymbol{X}}(\alpha) &= \sum_{k=0} \hat{\boldsymbol{A}}_k \alpha^k \\ \boldsymbol{I}(\boldsymbol{V}\hat{\boldsymbol{X}}) &= \sum_{k=0} \boldsymbol{A}_{I,k} \alpha^k \\ \boldsymbol{Q}(\boldsymbol{V}\hat{\boldsymbol{X}}) &= \sum_{k=0} \boldsymbol{A}_{Q,k} \alpha^k. \end{aligned} \tag{39}$$

Substituting from (39) into (14) and equating similar powers of α results in the following:

$$\hat{Y}\hat{\boldsymbol{A}}_1 + \boldsymbol{V}^T(\boldsymbol{A}_{I,1} + j\Omega \boldsymbol{A}_{Q,1} + \boldsymbol{I}_t) = 0 \tag{40}$$

$$\hat{Y}\hat{\boldsymbol{A}}_n + \boldsymbol{V}^T(\boldsymbol{A}_{I,n} + j\Omega \boldsymbol{A}_{Q,n}) = 0, \qquad n > 1. \tag{41}$$

Using the chain rule in differentiation, $\boldsymbol{A}_{I,1}$ in (40) can be written as

$$\begin{aligned} \boldsymbol{A}_{I,1} &= \frac{d}{d\alpha} \boldsymbol{I}\big(\boldsymbol{V}\hat{\boldsymbol{X}}(\alpha)\big) \\ &= \frac{\partial}{\partial \boldsymbol{X}} \big(\boldsymbol{I}(\boldsymbol{V}\hat{\boldsymbol{X}})\big) \frac{\partial \boldsymbol{X}}{\partial \hat{\boldsymbol{X}}} \frac{d}{d\alpha} \hat{\boldsymbol{X}} \\ &= \frac{\partial}{\partial \boldsymbol{X}} \big(\boldsymbol{I}(\boldsymbol{V}\hat{\boldsymbol{X}})\big) \boldsymbol{V} \frac{d}{d\alpha} \hat{\boldsymbol{X}}. \end{aligned} \tag{42}$$

Using the Taylor's expansion of $\hat{\boldsymbol{X}}(\alpha)$ in (39), (42) takes the form

$$\boldsymbol{A}_{I,1} = \frac{\partial}{\partial \boldsymbol{X}} \big(\boldsymbol{I}(\boldsymbol{V}\hat{\boldsymbol{X}})\big) \boldsymbol{V} \sum_{k=1} k \hat{\boldsymbol{A}}_k \alpha^{k-1}. \tag{43}$$

A similar expression for $\boldsymbol{A}_{Q,1}$ can also be obtained, where

$$\boldsymbol{A}_{Q,1} = \frac{\partial}{\partial \boldsymbol{X}} \big(\boldsymbol{Q}(\boldsymbol{V}\hat{\boldsymbol{X}})\big) \boldsymbol{V} \sum_{k=1} k \hat{\boldsymbol{A}}_k \alpha^{k-1}. \tag{44}$$

Using (26), (43), and (44), and substituting with $\alpha = 0$, (40) becomes

$$\boldsymbol{V}^T \boldsymbol{Y} \boldsymbol{V} \hat{\boldsymbol{A}}_1 + \boldsymbol{V}^T \boldsymbol{J}_0 \boldsymbol{V} \hat{\boldsymbol{A}}_1 + \boldsymbol{V}^T \boldsymbol{I}_t = 0. \tag{45}$$

Since $\boldsymbol{V}$ is an orthonormal basis for the subspace spanned by the columns of the matrix $[\boldsymbol{A}_0 \dots \boldsymbol{A}_q]$, it can then be represented in the form [9]

$$\boldsymbol{V} = [\boldsymbol{A}_0, \dots \boldsymbol{A}_q]\boldsymbol{R}^{-1} \tag{46}$$

where $\boldsymbol{R}$ is an upper triangular matrix. Substituting from (46) into (45) results in

$$\boldsymbol{K}^T\left(\boldsymbol{Y}[\boldsymbol{A}_0 \dots \boldsymbol{A}_q]\boldsymbol{R}^{-1}\hat{\boldsymbol{A}}_1 + \boldsymbol{J}_0[\boldsymbol{A}_0 \dots \boldsymbol{A}_q]\boldsymbol{R}^{-1}\hat{\boldsymbol{A}}_1 - \boldsymbol{I}_t\right) = 0 \tag{47}$$

where $\boldsymbol{K} = [\boldsymbol{A}_0 \dots \boldsymbol{A}_q]$. Substituting $\boldsymbol{R}^{-1}\hat{\boldsymbol{A}}_1 = \boldsymbol{e}_2$, where $\boldsymbol{e}_r$ is the rth column of the identity matrix, in (47) and simplifying yields

$$\boldsymbol{K}^T(\boldsymbol{Y}\boldsymbol{A}_1 + \boldsymbol{J}_0\boldsymbol{A}_1 - \boldsymbol{I}_t) = 0. \tag{48}$$

Hence, using (27), it can be seen that $\boldsymbol{R}^{-1}\hat{\boldsymbol{A}}_1 = \boldsymbol{e}_2$ is the solution for (47). Therefore, the mapping of $\hat{\boldsymbol{A}}_1$ through $\boldsymbol{V}$ produces

$$\boldsymbol{V}\hat{\boldsymbol{A}}_1 = \boldsymbol{K}\boldsymbol{R}^{-1}\hat{\boldsymbol{A}}_1 = [\boldsymbol{A}_0 \dots \boldsymbol{A}_q]\boldsymbol{e}_2 = \boldsymbol{A}_1 \tag{49}$$

Thus, it is clear from (49) that the first Taylor's series coefficient is preserved under a mapping by $\boldsymbol{V}$.

To proceed with higher derivatives, we write $\boldsymbol{A}_{I,n} + \boldsymbol{A}_{Q,n}$ in the form

$$\begin{aligned}\boldsymbol{A}_{I,n} + \boldsymbol{A}_{Q,n} &= \frac{1}{n!}\left(\frac{d^n}{d\alpha^n}\boldsymbol{I}(\boldsymbol{V}\hat{\boldsymbol{X}}(\alpha)) + j\Omega\frac{d^n}{d\alpha^n}(\boldsymbol{Q}(\boldsymbol{V}\hat{\boldsymbol{X}}(\alpha)))\right)\\ &= \frac{1}{n!}\frac{d^{n-1}}{d\alpha^{n-1}}\left(\boldsymbol{J}(\alpha)\left(\boldsymbol{V}\sum_{k=1}k\hat{\boldsymbol{A}}_k\alpha^{k-1}\right)\right).\end{aligned} \tag{50}$$

Substituting $\alpha = 0$ in the above equation and simplifying gives

$$\boldsymbol{A}_{I,n} + \boldsymbol{A}_{Q,n} = \frac{1}{n!}\sum_{j=1}^{n-1}\frac{(n-1)!}{(n-j-1)!}(n-j)!\left[\boldsymbol{J}_j(0)\right]\boldsymbol{V}\hat{\boldsymbol{A}}_{n-j}. \tag{51}$$

Now substitute from (51) into (41) to obtain

$$\boldsymbol{V}^T\left(\boldsymbol{Y}\boldsymbol{V}\hat{\boldsymbol{A}}_n + \boldsymbol{J}_0\boldsymbol{V}\hat{\boldsymbol{A}}_n + \sum_{j=1}^{n-1}\frac{(n-j)}{n}\left[\boldsymbol{J}_j(0)\right]\boldsymbol{V}\hat{\boldsymbol{A}}_{n-j}\right) = 0. \tag{52}$$

Now assume that $\boldsymbol{V}\hat{\boldsymbol{A}}_l = \boldsymbol{A}_l$ for $1 \le l \le n-1$ and use (46) in (52), we obtain

$$\boldsymbol{K}^T\left((\boldsymbol{Y} + \boldsymbol{J}_0)[\boldsymbol{A}_0 \dots \boldsymbol{A}_q]\boldsymbol{R}^{-1}\hat{\boldsymbol{A}}_n + \sum_{j=1}^{n-1}\frac{n-j}{n}\left[\boldsymbol{J}_j(0)\right]\boldsymbol{A}_{n-j}\right) = 0. \tag{53}$$

Substituting $\boldsymbol{R}^{-1}\hat{\boldsymbol{A}}_n = \boldsymbol{e}_{n+1}$ in the above equation yields

$$\boldsymbol{K}^T\left((\boldsymbol{Y} + \boldsymbol{J}_0)\boldsymbol{A}_n + \sum_{j=1}^{n-1}\frac{n-j}{n}\left[\boldsymbol{J}_j(0)\right]\boldsymbol{A}_{n-j}\right) = 0. \tag{54}$$

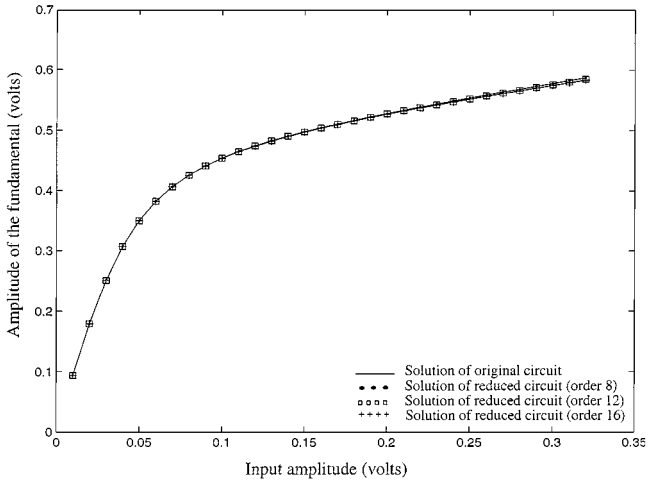

Fig. 1. Solution of the fundamental harmonic.

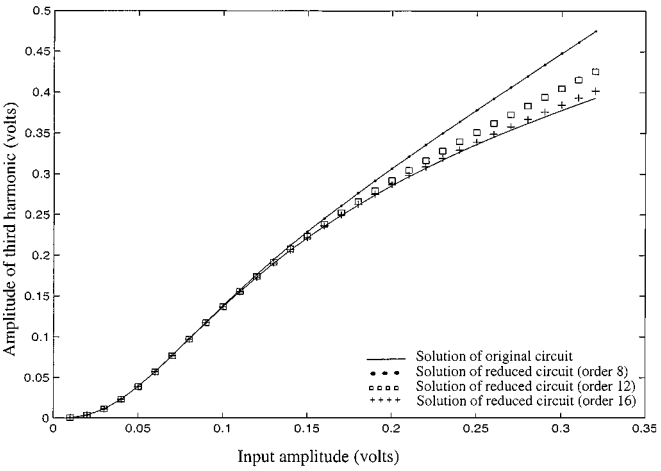

Fig. 2. Solution of the third harmonic.

Thus, comparing with (31) shows that $\boldsymbol{R}^{-1}\hat{\boldsymbol{A}}_n = \boldsymbol{e}_{n+1}$ is the solution for (53). Therefore, the mapping of $\hat{\boldsymbol{A}}$ through $\boldsymbol{V}$ produces

$$\boldsymbol{V}\hat{\boldsymbol{A}}_n = \boldsymbol{K}\boldsymbol{R}^{-1}\hat{\boldsymbol{A}}_n = [\boldsymbol{A}_0 \dots A_q]\boldsymbol{e}_{n+1} = \boldsymbol{A}_n. \tag{55}$$

Thus, it is clear from (55) that the nth Taylor's series coefficient is preserved under a mapping by $\boldsymbol{V}$. This completes the proof.

VI. Summary of the Algorithm

The main steps of the proposed algorithm are summarized as follows.

1) Starting from the dc operating point, the derivatives of the harmonics with respect to to α are computed as explained in Section IV
2) An orthonormal basis $\boldsymbol{V} \in \Re^{N(2H+1)\times q}$ for the column span of the derivatives matrix in (17) is constructed using QR factorization [12].
3) Using this orthonormal basis, a reduced system of nonlinear equations is formulated as in (14) and (15).
4) Equations (14) and (15) are solved for $\hat{\boldsymbol{X}}$ by incrementally increasing the value of $\alpha(0 \to 1)$

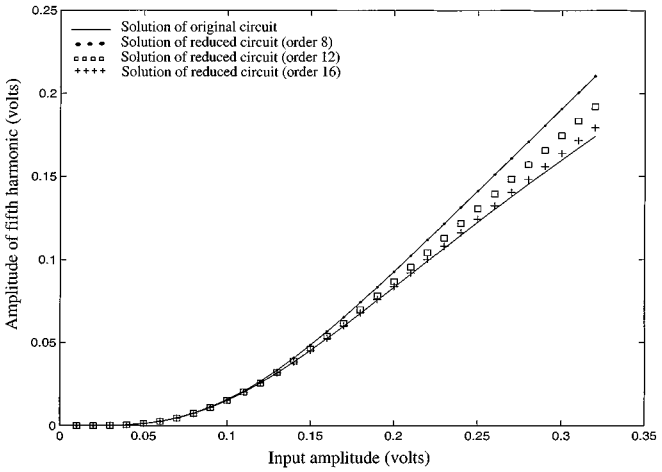

Fig. 3. Solution of the fifth harmonic.

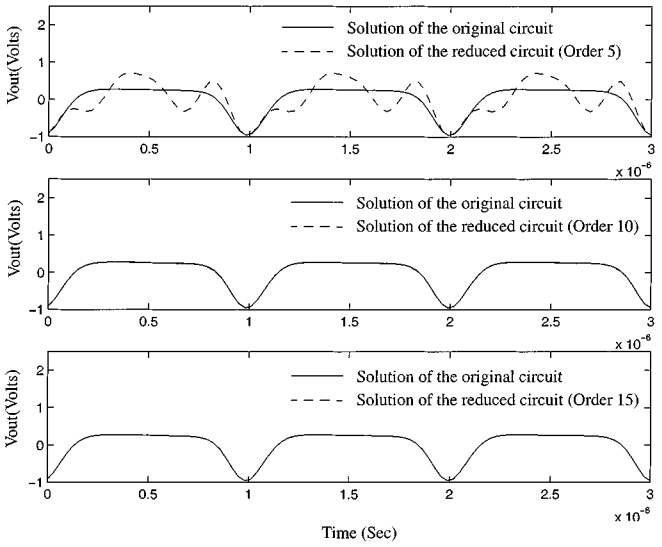

Fig. 4. Periodic time-domain response of the bipolar circuit (Example 1).

5) The solution of the original system is obtained in terms of $\hat{\boldsymbol{X}}$ using (13) and the residual error is calculated. The order of reduction q is increased if this residual error is greater than a prespecified tolerance.

VII. Numerical Examples

Example 1: The proposed circuit reduction technique was applied to a bipolar transistor amplifier circuit. The congruent transformation matrix was obtained from the derivatives at the dc solution, requiring only one LU factorization of the Jacobian matrix. The HB algorithm was then applied to the reduced circuit and the solution was compared with that of the original circuit. The output response as a function of the amplitude of the input waveform is shown in Figs. 1–3. As can be seen from the plots, a congruent transformation of order 16 is enough to match the response of the original circuit up to high distortion levels. The size of the Jacobian of the reduced circuit was only 16×16 compared with that of the original circuit Jacobian of 429×429. The proposed algorithm required only *one solution* of the large Jacobian equations. Conventional analysis, however, required this solution *63* times (one for each Newton iteration at each step of the continuation method). Fig. 4 shows a comparison for the time-domain response as obtained through solution of the original circuit using classical HB and the solution obtained through three different reduced circuits.

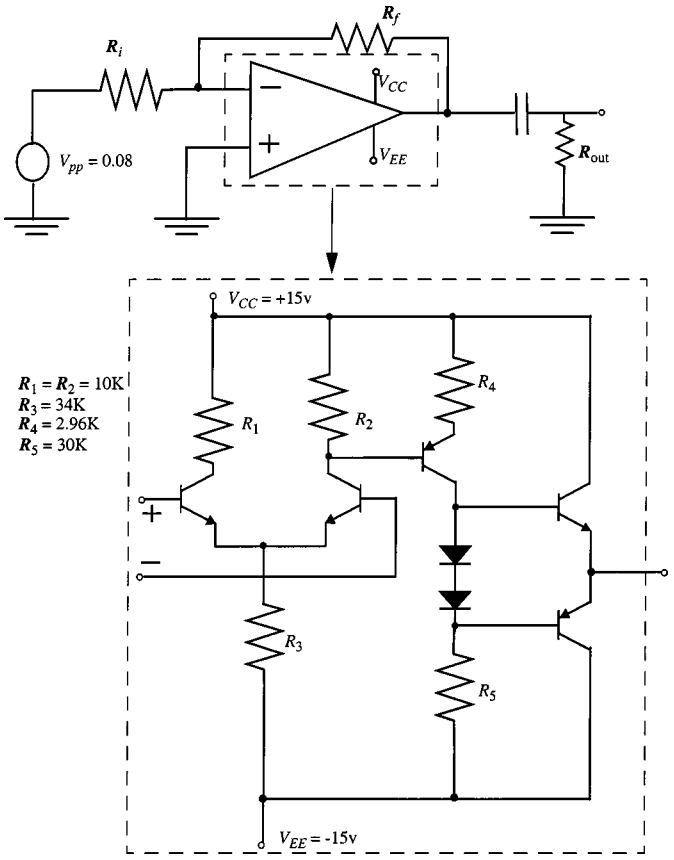

Fig. 5. Op–amp circuit of Example 2.

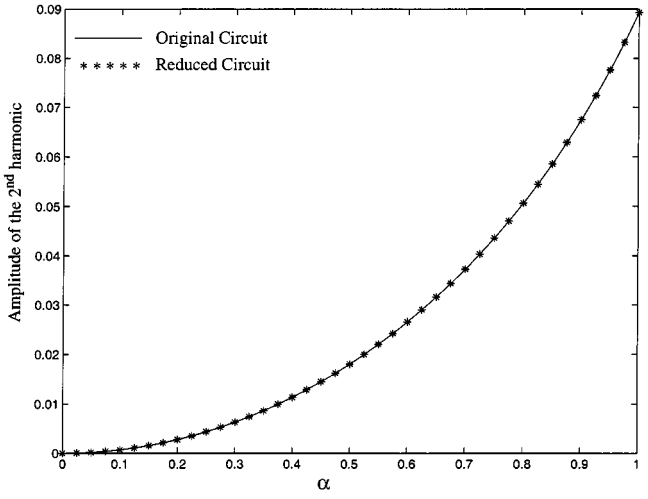

Fig. 6. Comparing the second harmonic behavior versus the continuation parameter α in the original and reduced circuit.

Example 2: An op–amp circuit consisting of five transistors is considered for this example (Fig. 5). Conventional HB analysis required 24 harmonics to approximate the steady-state response for this circuit. Performing the HB analysis needed 67

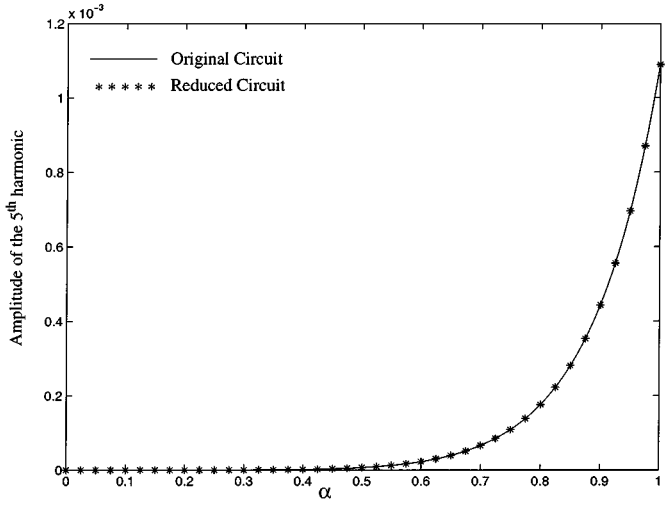

Fig. 7. Comparing the fifth harmonic behavior versus the continuation parameter α in the original and reduced circuit.

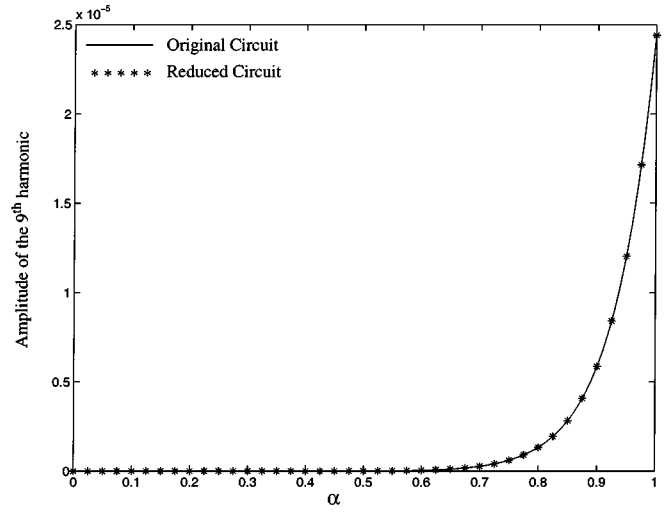

Fig. 8. Comparing the ninth harmonic behavior versus the continuation parameter α in the original and reduced circuit.

NR iterations with 67 LU decompositions of a Jacobian matrix of size 2400×2400.

Using the proposed algorithm, a reduced set of nonlinear equations of order 35 has been constructed using the derivatives at the dc operating point. Solution of the reduced set of nonlinear equations was then tracked versus the full swing of the input power. Figs. 6–8 depict the behavior of the second, fifth, and ninth harmonics of the output node voltage in both the original and reduced circuits versus the continuation parameter α. As can be seen, the behavior of the harmonics in the reduced system is indistinguishable from that of the original system. Fig. 9 shows a comparison for the magnitudes of the harmonics (in decibels per volt) at the output node as computed from the original and reduced circuits at the terminus of the continuation sweep $(\alpha = 1)$. A CPU comparison between the proposed algorithm and conventional HB is shown in Table II. As can be seen, a speedup factor of 12.3 was achieved without loss of accuracy.

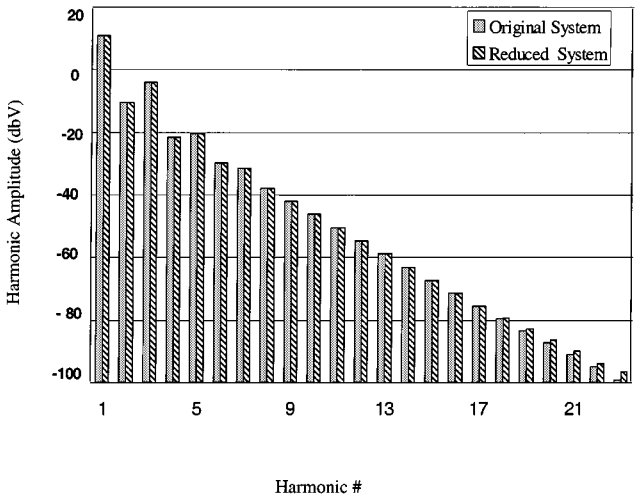

Fig. 9. Accuracy comparison.

TABLE II
CPU COMPARISON OF THE PROPOSED ALGORITHM VERSUS CONVENTIONAL HB

	Size of the Jacobian Matrix	CPU Time
Original Circuit	2400	388 (Sec)
Reduced Circuit	35	32 (Sec)

VIII. CONCLUSION

In this paper, a new algorithm for finding the steady-state solution has been proposed. The algorithm is based on the idea of nonlinear circuit reduction, where it uses a Krylov-based projection technique to construct a reduced set of nonlinear equations. The main feature of the reduced set of nonlinear equations is that it shares with the original HB equations the first derivatives with respect to the ac power of the input sources in the circuit at the dc operating point. Solution of the reduced set is then tracked through sweeping the power level of the input signal. The main advantage of the new algorithm is that reduces the size of the Jacobian matrix significantly, while preserving the accuracy of the solution. This results in a significant CPU cost savings.

Although most of the study here concentrated on a single-tone excitation circuits, the proposed algorithm can be applied in multitone situations as well. The advantage in this case will be even more conspicuous since the problem size becomes much bigger due to the increase number of spectral lines.

REFERENCES

[1] M. S. Nakhla and J. Vlach, "A piecewise harmonic balance technique for the determination of the periodic response of nonlinear systems," *IEEE Trans. Circuits Syst.*, vol. CAS-23, pp. 85–91, Feb. 1976.
[2] K. Kundert, J. White, and A. Sanjiovanni-Vincentilli, *Steady State Methods for Simulating Analog and Microwave Circuits*. Norwell, MA: Kluwer, 1990.
[3] K. Kundert, "Simulation methods for RF integrated circuits," in *ACM/IEEE Proc. ICCAD'97*, pp. 752–765.
[4] Y. Saad, *Iterative Methods for Sparse Linear Systems*. Boston, MA: PWS, 1996.
[5] D. Long, R. Melville, K. Ashby, and B. Horton, "Full-chip harmonic balance," in *Proc. IEEE CICC'97*, pp. 379–382.

[6] Y. Saad, *Iterative Methods for Sparse Linear Systems*. Boston, MA: ITP, 1996.
[7] S. Maas, *Nonlinear Microwave Circuits*. Norwood, MA: Artech House, 1988.
[8] E. Gad and M. Nakhla, "Model reduction for the DC solution of large nonlinear circuits," in *Proc. ICCAD'99*, pp. 376–379.
[9] G. H. Golub and C. Van Loan, *Matrix Computations*. Baltimore, MD: John Hopkins Univ. Press, 1989.
[10] J. W. Demmel, *Applied Numerical Linear Algebra*. Philadelphia, PA: SIAM, 1997.
[11] R. Griffith and M. S. Nakhla, "A new high order absolutely stable explicit numerical integration algorithm for the time-domain simulation of nonlinear circuits," in *Proc. IEEE/ACM ICCAD'97*, pp. 276–280.
[12] G. H. Golub and C. F. Van Loan, *Matrix Computations*. Baltimore, MD: John Hopkins Univ. Press, 1989.

Emad Gad (S'99) was born in 1969. He received the B.E. degree from Alexandria University, Alexandria, Egypt, in 1991, the M.E. degree from Cairo University, Cairo, Egypt, in 1997, and is currently working toward the Ph.D. degree on developing model reduction algorithms for efficient simulation of linear and nonlinear circuits at Carleton University, Ottawa, ON, Canada.

His main research interests are circuit simulation, numerical algorithms, and learning theory.

Mr. Gad was the recipient of the 1999 Ontario Graduate Students Scholarship, the 1999–2000 Ontario Graduate Scholarship in Science and Technology, and the 2000–20001 Ontario Graduate Scholarship.

Roni Khazaka (S'92) was born in 1973. He received the B.E. and M.E. degrees from Carleton University, Ottawa, ON, Canada, in 1995 and 1997 respectively, and is currently working toward the Ph.D. degree on model-reduction techniques for nonlinear and linear circuit simulation at Carleton University.

He has co-authored several papers on the simulation of high-speed interconnects and RF circuits, and spent a term at Nortel Networks, where he developed a prototype system-level simulation tool. His current research interests include the analysis and simulation of RF ICs and high-speed interconnects.

Mr. Khazaka was the recipient of the Natural Sciences and Engineering Research Council Scholarship (at the masters and doctoral levels) and the IBM Cooperative Fellowship.

Michel S. Nakhla (S'73–M'75–SM'88–F'98) received the M.Eng. and Ph.D. degrees in electrical engineering from Waterloo University, Waterloo, ON, Canada, in 1973 and 1975, respectively.

From 1976 to 1988, he was with Bell-Northern Research (currently Nortel Networks), as the Senior Manager of the Computer-Aided Engineering Group. In 1988, he joined Carleton University, Ottawa, ON, Canada, where he is currently the Holder of the Computer Aided Engineering Senior Industrial Chair, established by Bell-Northern Research and the Natural Sciences and Engineering Research Council of Canada. He is also currently a Professor of electrical engineering, and founder of the High-Speed Computer-Aided Design (CAD) Research Group. He is a technical consultant for several industrial organizations and the principal investigator for several major sponsored research projects. His research interests include CAD of very large scale integration (VLSI) and microwave circuits, modeling and simulation of high-speed interconnects, nonlinear circuits, multidisciplinary optimization, thermal and electromagnetic (EM) emission analysis, noise analysis, mixed EM/circuit simulation, wavelets, and neural networks.

Richard Griffith (S'92) received the B.Eng. degree in electrical engineering from Lakehead University, Thunder Bay, ON, Canada, in 1986, the M.Eng. degree from Carleton University, Ottawa, ON, Canada, in 1997, and is currently working toward the Ph.D. degree in electronics at Carleton University.

He was a Research Engineer at Carleton University, Ottawa, ON, Canada. His research interests are VLSI CAD and numerical algorithms.